CHAPTER 5 FUZZY LOGIC CONTROL APPLICATION FOR MAGNETIC LEVITATION SYSTEM

Magnetic levitation is achieved when a metal object is suspended in air with the help of electromagnetic force. Magnetic levitation (maglev) has numerous applications: magnetic bearings [100], maglev trains [101], magnetic conveyer belts [102], complicated maglev based space propulsion [103]. A simple magnetic levitation system is depicted in Figure 5-1. Here an electromagnet levitates a steel ball. The current passing through electromagnet can be varied to control the magnetic force which controls the steel ball position. The current in electromagnet is varied by using a voltage to current converter.

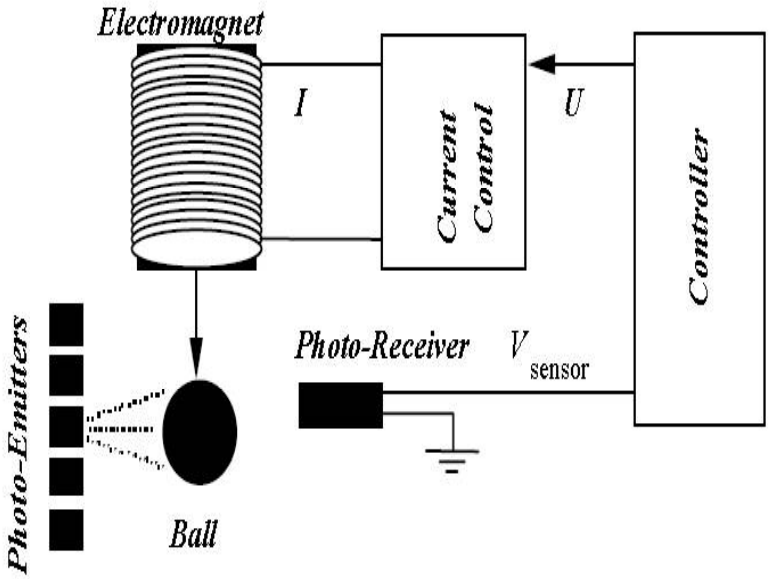

Figure 5-1 Magnetic levitation of steel ball

This chapter discusses the implementation for proposed controller for control of steel ball position using maglev. The proposed controller performance when compared to performance of PID control and fuzzy logic control for following parameters:

- Transient response parameters: peak overshoot.
- Steady – state error.
- Performance indices.

5. 1 Problem formulation

The control objective for steel ball position control is: "to generate the electromagnetic force to counteract the gravitational force acting on the ball so

as to maintain the steel ball at desired position". The air gap between electromagnet and steel ball introduces nose into the system, thereby increasing the uncertainty in the system. The fuzzy logic being robust to system uncertainty results in increased noise immunity for the system thereby decreasing the sensitivity. This improves the accuracy and response speed for the controller. Since fuzzy controller for maglev is created considering the system as black box system the resulting controller handles the system non-linearity and uncertainty efficiently.

The hardware employed for experimental purpose is developed by Feedback Instruments ltd™ as illustrated in Figure 5-2.

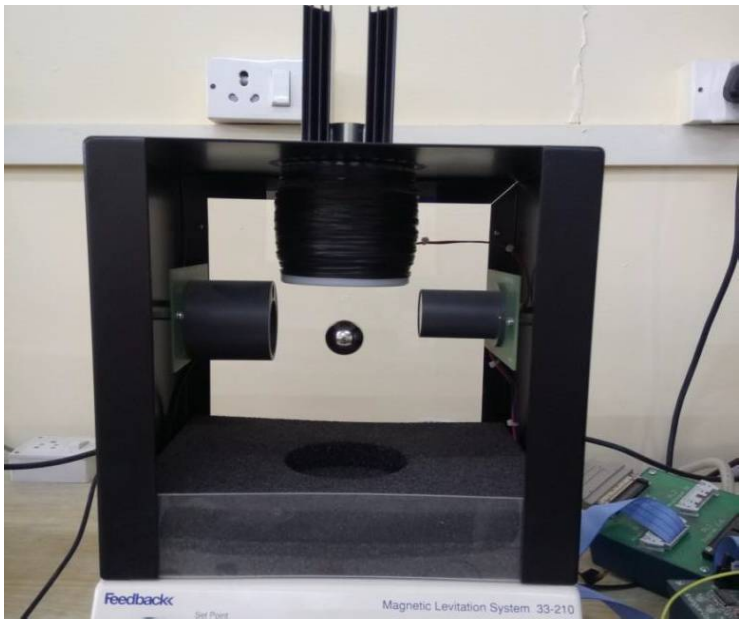

Figure 5-2 Real-time magnetic levitation model available in Control theory and simulation lab, UPES

The maglev is connected to computer via a DAQ card. The DAQ card acts as a real-time interface device between the analog maglev system and digital computer. Analog signals generated form position sensor is converted to digital signals for transmission to PC. Similarly digital signals generated by PC (via Matlab-Simulink™) are converted to analog signals via the DAQ card.

5. 2 Mathematical modeling

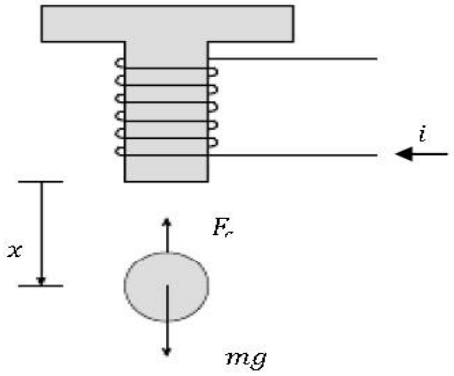

Figure 5-3 Forces acting on steel ball

Forces acting in the system can be noted from Figure 5-3. To suspend the stell ball to a desired position, the force generated by electromagnet has to balance the ball weight. Mathematically:

$$F_a = F_m - mg \tag{5-1}$$

here, $F_a$is: resultant force experienced by steel ball, $F_m$is the magnetic force, m is mass of the steel ball, g: acceleration due to gravity.Tthe equation can be depicted as:

$$m\ddot{x} = mg - f(i,x) \tag{5-2}$$

here, x is: displacement of ball from its reference position, k is: system constant depending on the coil used.

$$f(i,x) = C\frac{i^2(t)}{x^2(t)} \tag{5-3}$$

here, C is: force constant = $\frac{L_0 x_0}{2}$, L_0 is the incremental inductance of coil with ball and x_0 is: incremental displacement of the steel ball.

The hardware model utilized for real-time experiment consists of an inner control loop which produces a coil current proportional to input control voltage:

$$i = k_1.u \tag{5-4}$$

The linear state-space model for maglev can be depicted as:

$$\begin{bmatrix}\dot{x}_1\\ \dot{x}_2\\ y\end{bmatrix} = \begin{bmatrix}x_2\\ g - \frac{kk_1^2u^2}{mx_1^2}\\ k_2x_1\end{bmatrix} \tag{5-5}$$

The system parameters for real-time model are depicted in Table 5-1

Table 5-1 Parameters of the physical model used

Symbol	Description	Value
x	Ball position	[0.005, 0.025]m
i	Coil current	[0,3]A
u	Control voltage (input voltage for coil)	[0,5]V
m	Mass of steel ball	*0.02 Kg*
k	Coil magnetic const.	$8.24\times10^{-5}Nm^2/A^2$
k_1	I/P conductance	0.397 /Ω
k_2	Conversion coefficient	100 V/m
g	Acceleration due to gravity	9.8 m/s^2

5. 3 Fuzzy logic control

The fuzzy logic control architecture for maglev is illustrated in Figure 5-4.

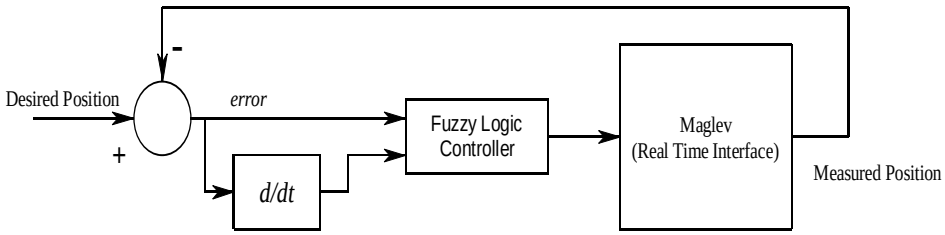

Figure 5-4 Fuzzy logic control for Magnetic levitation system

As can be seen in figure the fuzzy controller used here is of PD type. The DAQ card acts as a real-time interface device between the "analog system" and the "digital computer". The position sensors generate analog signals which are converted to digital signals via DAQ card. Similarly the digital control signal generated by PC via Matlab-Simulink™ is converted to analog signal via the DAQ card.

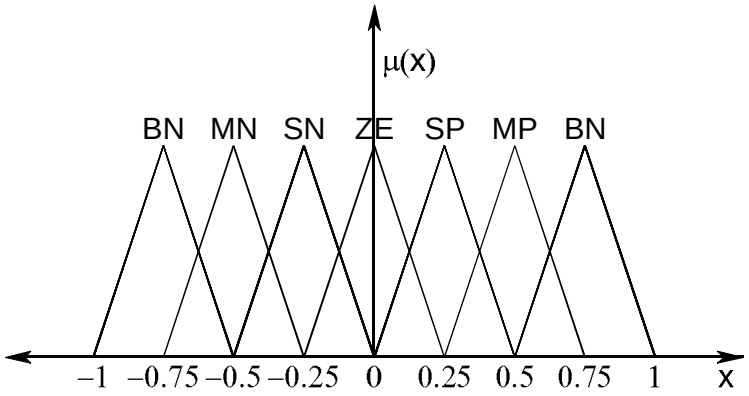

Figure 5-5 Initial FS for error

The initial FS designed for maglev fuzzy logic control can be seen in Figure 5-5. The sets are designed according to the procedure discussed in section 2. 4. Here the fuzzy sets are named on their relative location with zero error. FS for the "$\dot{e}$" and "c" are designed using same principle. The range for these sets is:

$$\dot{e} = [-10, 10] \qquad c = [0, 5]$$

Table 5-2 describes the rule base for maglev fuzzy controller:

Table 5-2 Rule base for ball position error, rate of change of error and Control signal

Control voltage		Rate of change of error ($\dot{e}$)						
		BN	MN	SN	ZE	SP	MP	BP
Error in position (e)	BN	BN	BN	BN	BN	MN	SN	ZE
	MN	BN	BN	BN	MN	SN	ZE	SP
	SN	BN	BN	MN	SN	ZE	SP	MP
	ZE	BN	MN	SN	ZE	SP	MP	BP
	SP	MN	SN	ZE	SP	MP	BP	BP
	MP	SN	ZE	SP	MP	BP	BP	BP
	BP	ZE	PS	PM	BP	BP	BP	BP

These rules are an extension from the control perspective discussed in section 5. 1.

5. 3. 1 Optimized fuzzy logic control

For optimization process the displaced FSs are employed to obtain optimized FS. Considering data obtained for ball position error we proceed to find optimized set for position error and in a similar way for ($\dot{e}$) and (c)Standard deviation (σ) calculated are:

$\sigma_e = 0.2$ $\sigma_{\dot{e}} = 4.3$ $\sigma_c = 1.4$

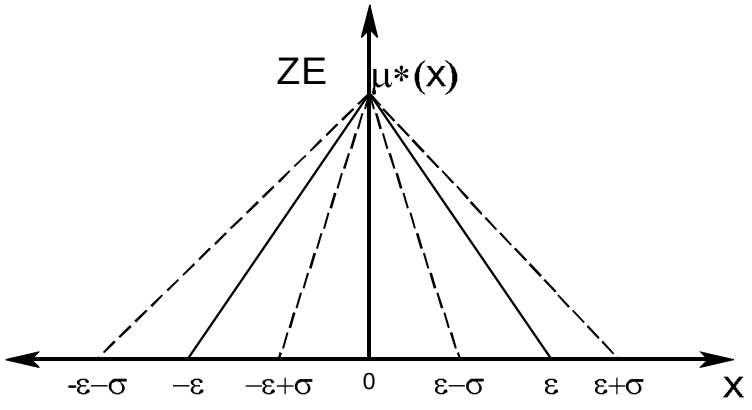

Figure 5-6 FS of position error for set "ze"

Figure 5-6 depicts a displaced FS "Zero".

Following objective function is used to obtain optimized FS.

$$\text{Maximize } H(A) = \int_a^b f\left(\frac{x-a}{b-a}\right)dx + \int_b^c f\left(\frac{x-c}{b-c}\right)dx \quad \text{Subject to maximum } H(\mu) = \sum_{i=1}^{n} H(\mu_i) \tag{5-6}$$

The next step to obtain the optimized fuzzy sets is to find the optimized value of the objective function stated above and compute the support for predefined sets. The objective function for FS "Zero" is shown as an example

Maximize

$$H(\mu_{Z^*}) = -\left[\int_{-\varepsilon\mp\sigma}^{0}\left(\frac{x+\varepsilon\mp\sigma}{\varepsilon\mp\sigma}\right)ln\left(\frac{x+\varepsilon\mp\sigma}{\varepsilon\mp\sigma}\right)dx + \int_{-\varepsilon\mp\sigma}^{0}\left(-\frac{x}{\varepsilon\mp\varepsilon}\right)ln\left(-\frac{x}{\varepsilon\mp\varepsilon}\right)dx\right] - \left[\int_{0}^{\varepsilon\pm\sigma}\left(\frac{\varepsilon\pm\sigma-x}{\varepsilon\pm\sigma}\right)ln\left(\frac{\varepsilon\pm\sigma-x}{\varepsilon\pm\sigma}\right)dx + \int_{0}^{\varepsilon\pm\sigma}\left(\frac{x}{\varepsilon\pm\sigma}\right)ln\left(\frac{x}{\varepsilon\pm\sigma}\right)dx\right] \tag{5-7}$$

Subject to maximum $H(\mu) = \sum_{i=1}^{n} H(\mu_i)$

5. 4 Simulation model and real-time experiment results

Figure 5-7 depicts the simulation model of magnetic levitation system. This simulation model is designed for the linear model. PID gains are tuned for the linear maglev model. The input to the controller is the error and is calculated as the difference of desired set-point and measured position:

$$e = y_{sp} - y_m \tag{5-8}$$

PID controller generates an output to minimize error. The control voltage obtained is further converted to a corresponding current by using a voltage-to-current converter. The results depicted here are obtained for real-time hardware model depicted in Figure 5-2. Here, the PID controller is designed for the linearized model and is then implemented for control of the real-time non-linear model. The PID gains are obtained using the optimized Zeigler-Nichols (ZN) tuning method. Here, PID gains are initially obtained using ZN tuning which are further optimized for least error-indices. This is computed from simulation model.

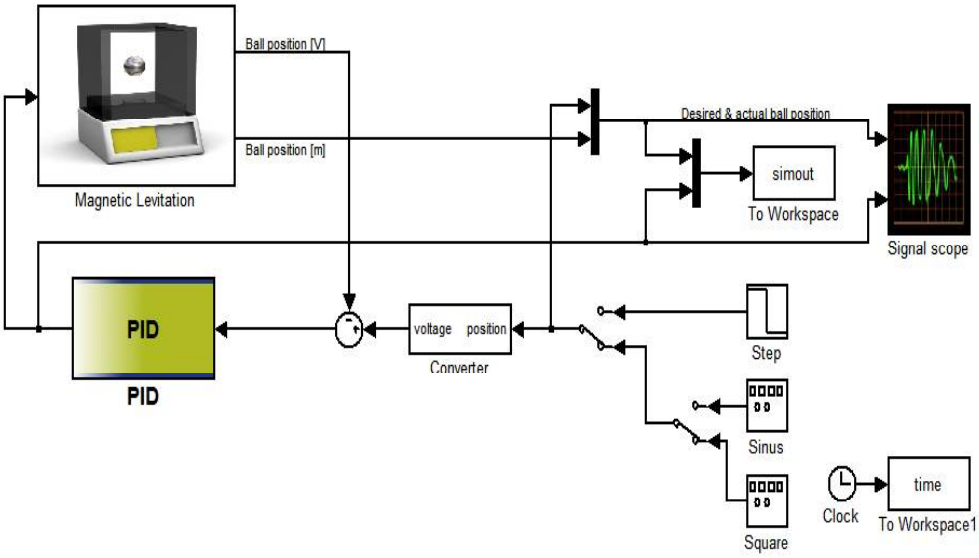

Figure 5-7 Simulation model for magnetic levitation system

5. 4. 1 Real-time PID control

Figure 5-8 depicts the architecture for PID control of real time maglev system. The PID parameters are tuned for generalized system, i.e. for a broad range of operating points.

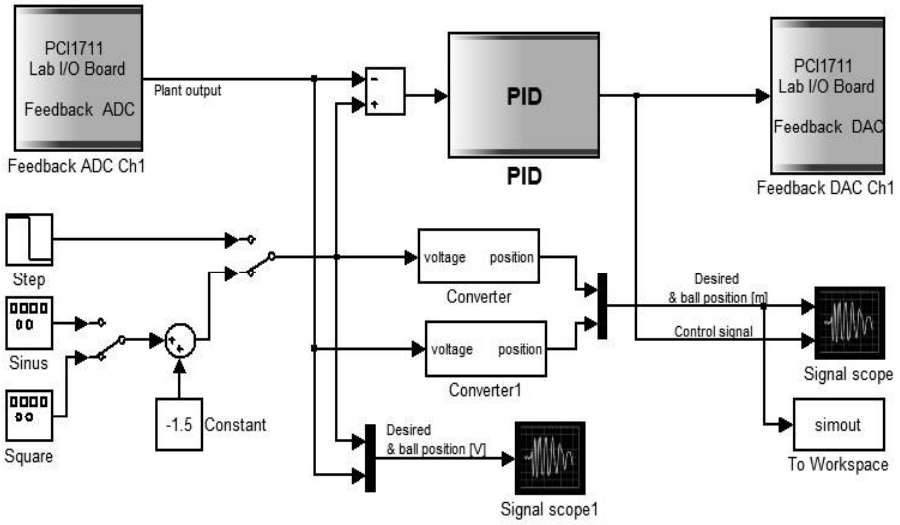

Figure 5-8 PID control for magnetic levitation **[104]**

Figure 5-9 depicts the PID controller response for step change in desired ball position with 0 initial conditions, and a reference position of 9mm is provided as desired position for 5 seconds, following which it is changed to a 5.5mm for next 5 seconds.

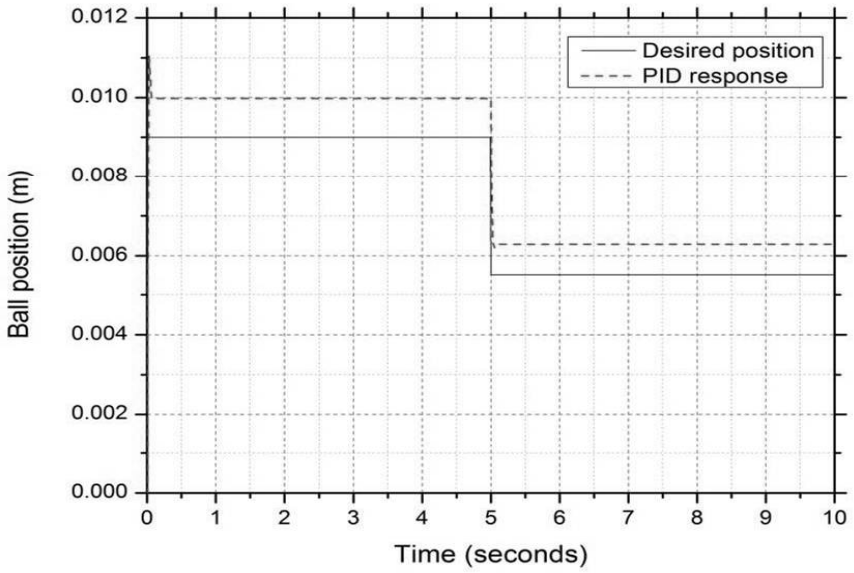

Figure 5-9 PID controller response for step change in ball position

Here the steady-state error exhibited by controller is 1mm (11.11%) for initial reference value of 9mm. than the steady-state error changes to 0.8 mm (14.54%) for reference value of 5.5mm. non-zero steady-state error is due to the loss of generalization when the system is linearized. Table 5-3 depicts the error indices for PID controller.

Table 5-3 Performance indices for PID controller with unit step set-point change

Error indices	ISE	ITSE	IAE	ITAE
PID Control	1.431	7.845	3.726	14.21

Furthermore a sinusoidal set-point is applied to the system in order to evaluate its dynamic performance. The sinusoidal set-point has a peak value of ±5mm for ball position. Figure 5-10 depicts the response for PID controller. Being a sinusoidal set-point we cannot comment on the steady-state error, hence error at (a) positive peak is 0.7mm (14%), and at (b) negative peak is 0.2mm (4%). Table 5-4 summarizes the performance indices for the same.

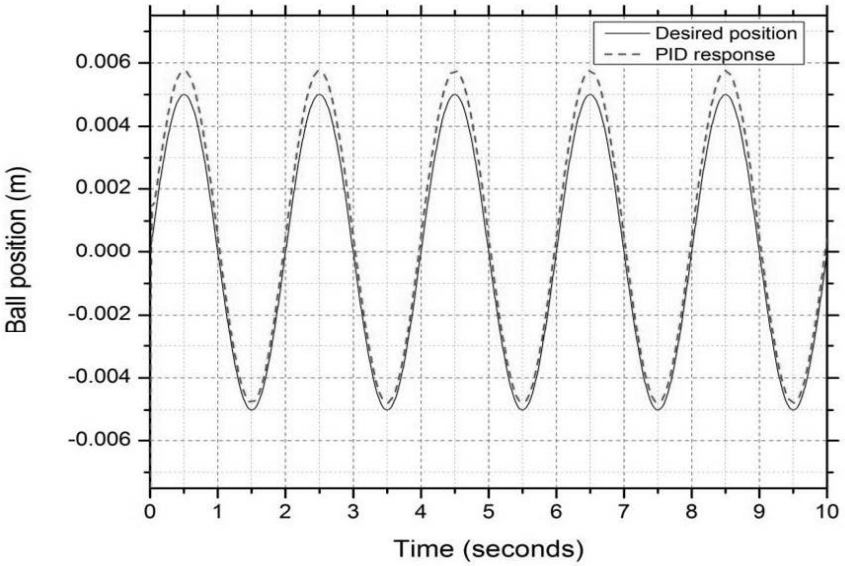

Figure 5-10 PID controller response for sinusoidal change in ball position

Table 5-4 Performance indices for PID controller with sinusoidal set-point change

Error indices	ISE	ITSE	IAE	ITAE
PID Control	0.6629	3.038	2.374	11.42

5. 4. 2 Real-time fuzzy logic control

This section discusses the response for FLC, the architecture of FLC is depicted in Figure 5-4.

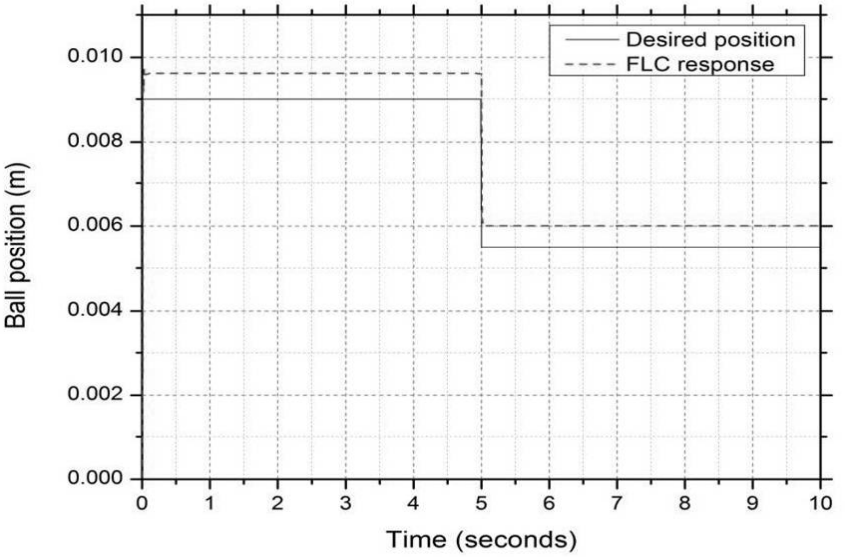

Figure 5-11 FLC response for step change in ball position

The response for FLC is evaluated using same series of set-points for which PID response is evaluated. Figure 5-11 depicts the FLC response for step change in desired ball position set-point with 0 initial conditions, and a 9mm reference position. The steady-state error for FLC is 0.62mm (6.89%).

Following which the set-point is now changed to reference value of 5.5mm for next 5 seconds, here the steady-state error exhibited by controller is 0.5mm (9.09%). Table 5-5 summarizes the performance indices for the same.

Table 5-5 Performance indices for PID controller with unit step set-point change

Error indices	ISE	ITSE	IAE	ITAE
FLC	0.6508	1.8626	1.926	6.078

FLC response to sinusoidal changes in desired position is given in Figure 5-12. The sinusoidal set-point has a peak value of ±5mm for ball position. Being a sinusoidal set-point we cannot comment on the steady-state error but the error at (a) positive peak is 0.5mm (10%), and at (b) negative peak is 0.1mm (2%). Table 5-6 summarizes the performance indices for the same.

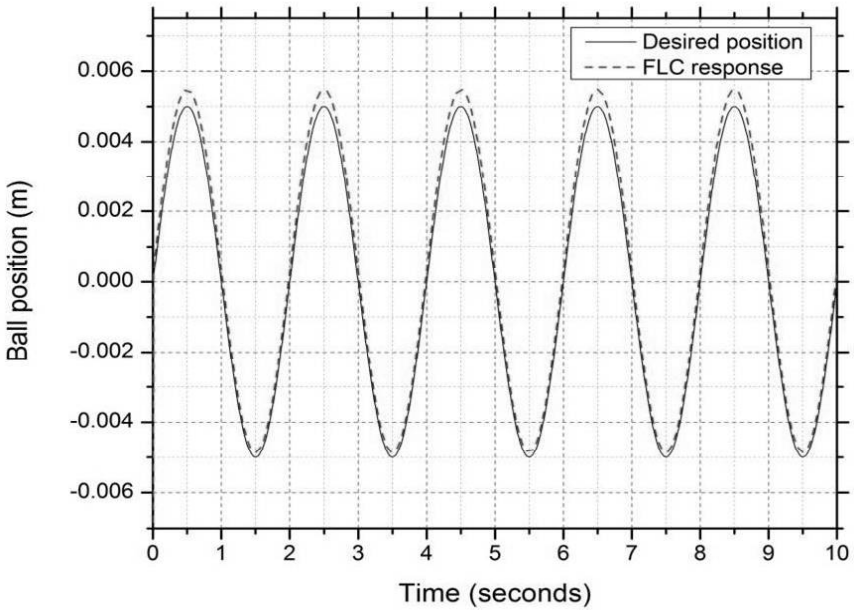

Figure 5-12 FLC response for sinusoidal change in ball position

Table 5-6 Performance indices for FLC with sinusoidal set-point change

Error indices	ISE	ITSE	IAE	ITAE
FLC	0.07731	0.2682	0.7244	3.391

5. 4. 3 Real-time optimized fuzzy logic control

The optimized values for FSs are calculated employing optimization algorithm after which the optimized controller is implemented for real-time control. The response for proposed controller is evaluated for the same set-points for which PID and FLC response are evaluated. Figure 5-13 depicts the response for optimized FLC response to step change in desired ball position with 0 initial

conditions, and a reference position of 9mm is now given as the set-point for 5 seconds. Now the steady-state error exhibited by optimized FLC is 0.2mm (2.22%). Following this the reference position is changed to 5.5mm for next 5 seconds, here the steady-state error exhibited by controller is 0.02mm (.036%). Table 5-7 summarizes the performance indices for the same.

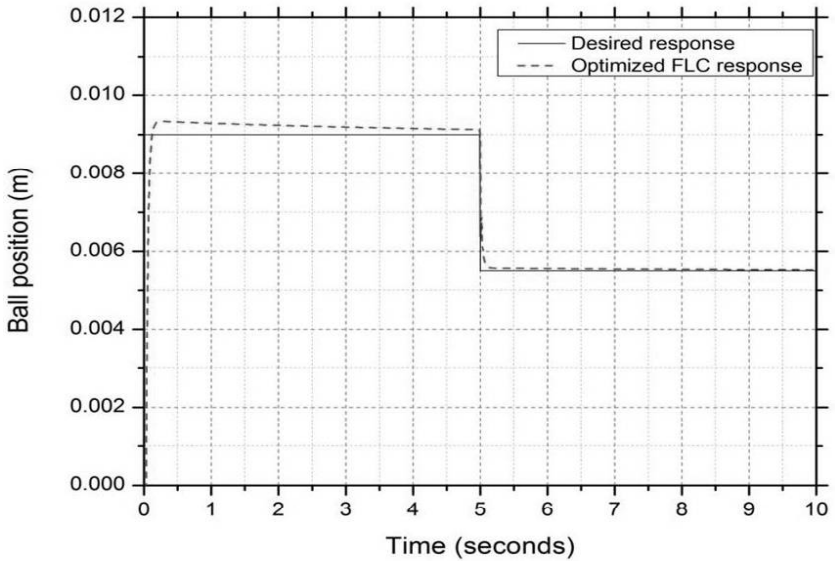

Figure 5-13 Optimized FLC response for step change in ball position

Table 5-7 Performance indices for optimized PID controller with unit step set-point change

Error indices	ISE	ITSE	IAE	ITAE
Optimized FLC	0.1007	0.08187	0.4356	1.8

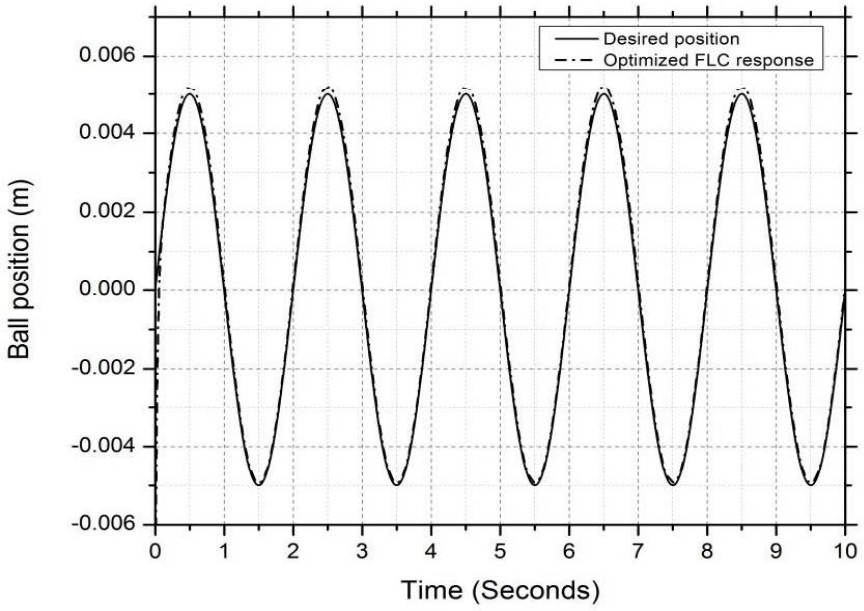

Figure 5-14 FLC response for step change in ball position

Optimized FLC response to sinusoidal changes in desired position is given in Figure 5-14. The sinusoidal set-point has a peak value of ±5mm for ball position. Being a sinusoidal set-point we cannot comment on the steady-state error, however the error at (a) positive peak is 0.125mm (2.5%), and at (b) negative peak is 0mm (0%). Table 5-8 summarizes the performance indices for the same.

Table 5-8 Performance indices for PID controller with sinusoidal set-point change

Error indices	ISE	ITSE	IAE	ITAE
Optimized FLC	0.02553	0.02263	0.231	0.9803

5. 5 Comparative analysis

Figure 5-15 depicts the response for PID, FLC and proposed controller to step change in ball desired position. The system initial condition is set at 0, and a reference position of 9mm is given for 5 seconds. Here the steady-state error exhibited by: (a) PID controller is 1mm (11.11%), (b) FLC is 0.62mm (6.89%), and (c) Optimized FLC is 0.2mm (2.22%). Following which the reference value is now changed to 5.5mm for next 5 seconds. Here the steady-state error exhibited by: (a) PID controller is 0.8 mm (14.54%), (b) FLC is 0.5mm (9.09%), and (c) Optimized FLC is 0.02mm (0.36%).

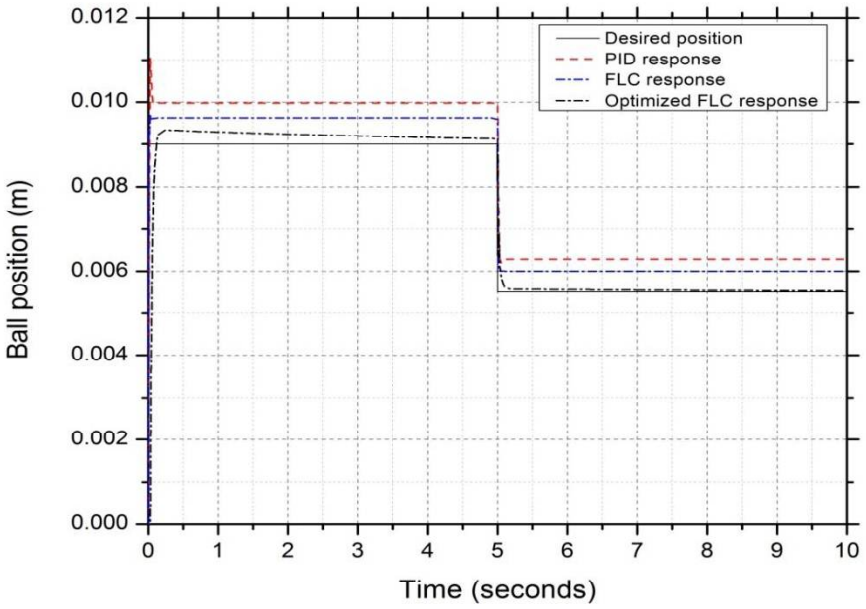

Figure 5-15 Performance comparison for PID, FLC and optimized FLC for step changes in desired position

Table 5-9 summarizes the steady-state error values and error indices for PID, FLC, and optimized FLC controllers which indicate a low value for parameters for the optimized fuzzy logic controller as compared with PID or FLC.

Table 5-9 Error indices comparison for PID, FLC and optimized FLC for step changes in desired position

Parameter	PID	FLC	Optimized FLC
Error (first step change)	0.001 m	0.00062 m	0.0002 m
Error (second step change)	0.008 m	0.0005 m	0.00002 m
ISE	1.431	0.6508	0.1007
ITSE	7.845	1.8626	0.8187
IAE	3.726	1.926	0.4356
ITAE	14.21	6.078	1.8

Figure 5-16 depicts the response for PID, FLC & optimized FLC for sinusoidal change in desired ball position. The system initial condition is set at 0, and a sinusoidal set-point has a peak value of ±5mm for ball position. For positive peak the error exhibited by: (a) PID controller is 0.7mm (14%), (b) FLC is 0.5mm (10%), and (c) Optimized FLC is 0.125mm (2.5%). For negative peak the error exhibited by: (a) PID controller is 0.2 mm (4%), (b) FLC is 0.1mm (2%), and (c) Optimized FLC is 0mm (0%).

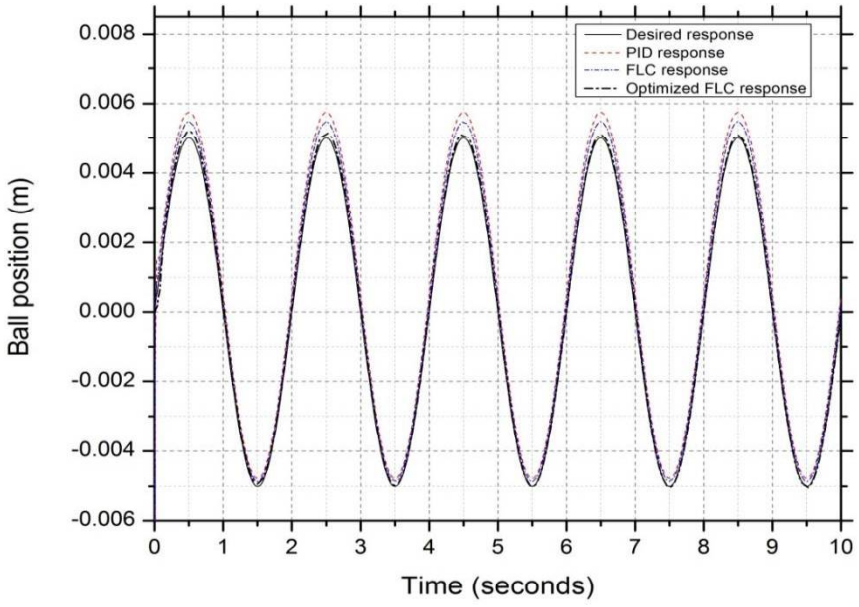

Figure 5-16 Performance comparison for PID, FLC and optimized FLC for sinusoidal change in desired position

Table 5-10 summarizes the steady-state error values and error indices for PID, FLC, and optimized FLC controllers.

Table 5-10 Error indices comparison for PID, FLC and optimized FLC for step changes in desired position

Parameter	PID	FLC	Optimized FLC
Error (positive peak)	14%	10%	2.5%
Error (negative peak)	4%	2%	0%
ISE	0.6629	0.07731	0.02553
ITSE	3.038	0.2682	0.02263
IAE	2.374	0.7244	0.231
ITAE	11.42	3.391	0.9803

Results for real time experiments indicate an improvement in; transient, steady-state response parameters and error indices for optimized FLC as compared with PID controller or FLC.

5. 5. 1 Comparison of proposed controller with referenced work

The Performance for proposed controller is also compared with some reference controllers which employ FLC for steel ball maglev control. Lee et.al [105] employed a two-input single-output FLC using a α, β prefilter for measurement uncertainty and noise removal. Considering a PD type fuzzy controller the α, β fuzzy controller architecture is depicted in Figure 5-17.

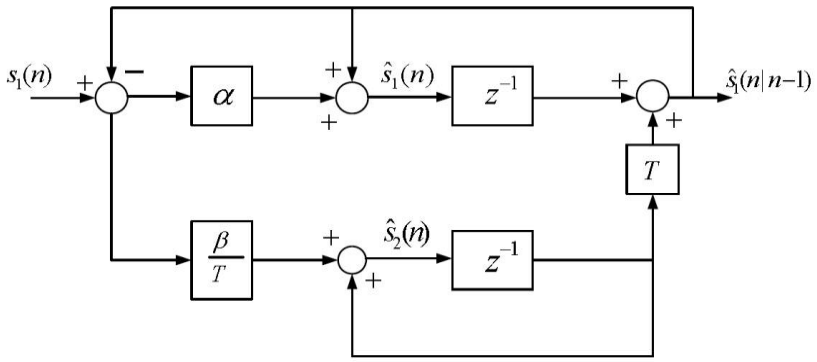

Figure 5-17 Architecture of alpha-beta filter FLC

where $S_1(n)$ represents the error, $S_1(n-1)$ represents the differential error, T represents sampling time. α, β are calculates as per the Benedict and Bordner [106] criteria:

$$\beta = \frac{\alpha^2}{(2-\alpha)} \tag{5-9}$$

α is determined using the desired variance reduction ratio (VRR):

$$VRR = \frac{\alpha(6-5\alpha)}{\alpha^2 - 8\alpha + 8} \tag{5-10}$$

Figure 5-18 depicts comparison for step change in desired ball position for (a) proposed controller with (b) Lee's α, β filter based fuzzy controller.

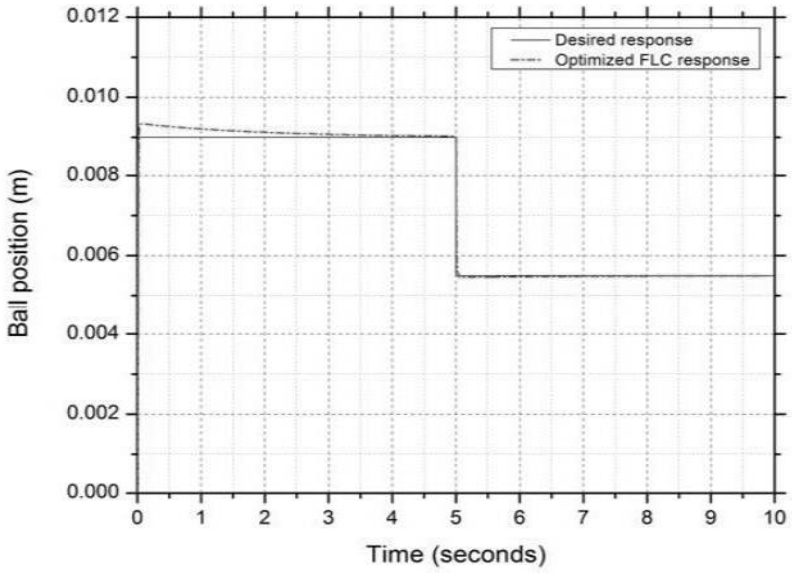

(a)

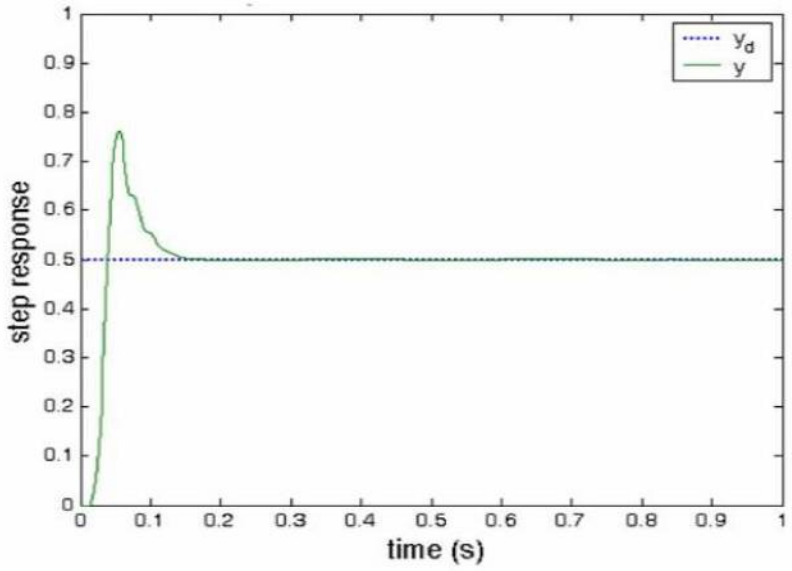

(b)

Figure 5-18 Step change in ball position response for (a) proposed controller (b) reference controller **[105]**

Table 5-11 illustrates comparison of peak overshoot for (a) proposed controller with (b) Lee's α, β filter based fuzzy controller.

Table 5-11 Performance comparison for step changes in desired ball position

Controller	Peak Overshoot	Steady-state error
Proposed controller	4.25%	0mm
α, β filter based FLC [105]	35.4%	0mm

Golob et.al. [39] applied two distinct decomposed PID fuzzy controllers for maglev control of ball position. These controllers are:

$$de(k) = \frac{e(k) - e(k-1)}{T} \tag{5-11}$$

$$ie(k) = ie(k-1) + Te(k-1) \tag{5-12}$$

where $e(k)$is the error, $de(k)$ is differential of error , $ie(k)$ is accumulated error, T is sampling time. These controllers are: (a) fuzzy PID controller, and (b) fuzzy PD+PI controller. The controller architecture are depicted in Figure 5-19 and Figure 5-20.respectively.

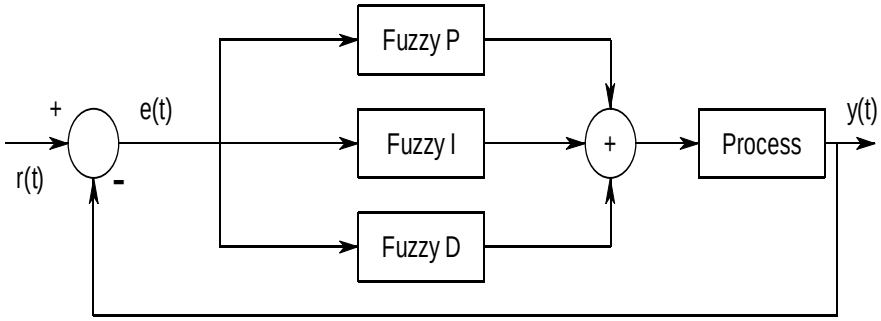

Figure 5-19 Decomposed fuzzy PID controller

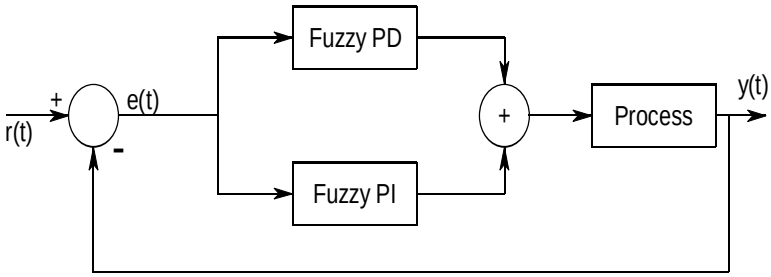

Figure 5-20 Decomposed fuzzy PID controller

Figure 5-21 depicts comparison for step change in ball's desired position for (a) proposed controller with (b) decomposed fuzzy controllers. Table 5-12 illustrates the comparison of overshoot for comparison of the step change in desired ball position for (a) proposed controller with (b) decomposed fuzzy controllers.

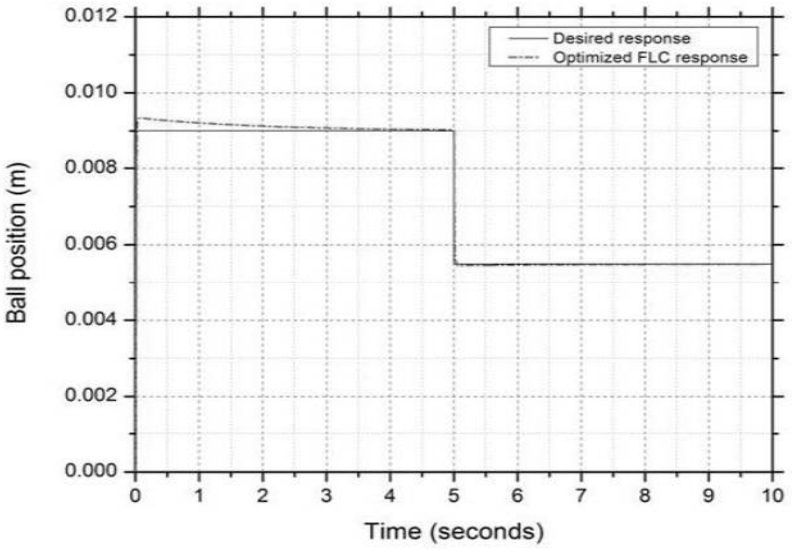

(a)

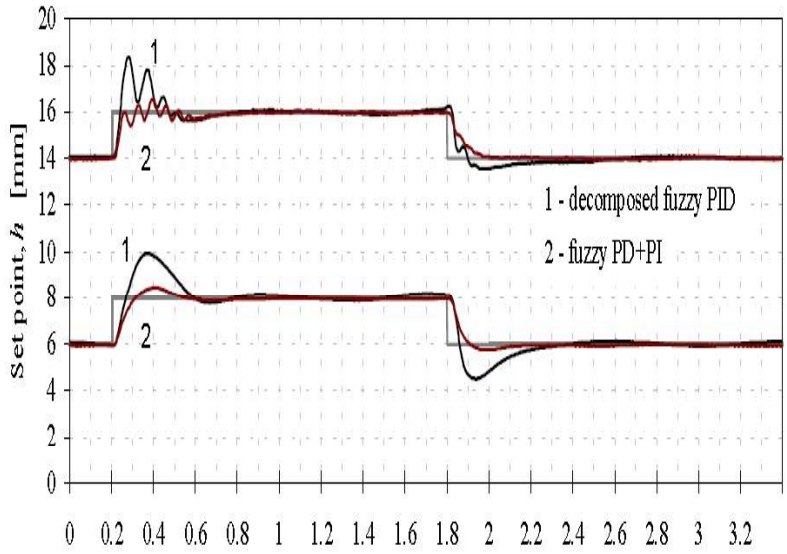

(b)

Figure 5-21 Step change in ball position response for (a) proposed controller (b) reference controller **[105]**

Table 5-12 Performance comparison for step changes in desired ball position

Controller	Peak Overshoot	Steady-state error
Proposed controller	4.251%	0mm
Decomposed fuzzy PID	12.8%	0mm
Fuzzy PD+PI	5.8%	0mm

5. 6 Conclusion

This chapter covers the real-time control for magnetic levitation system is used. The performance comparison for optimized controller is summarized in this section.

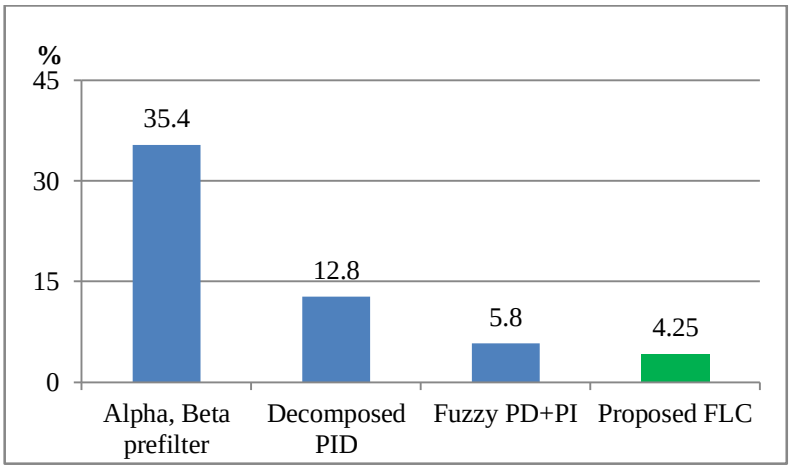

Figure 5-22 Overshoot comparison of proposed controller with reference controllers

Figure 5-22 illustrates comparison of overshoot for proposed controller with reference controllers. The proposed controller exhibits a reduction of 31.15% in peak overshoot when compared with Lee's [105] prefilter based FLC. The proposed controller exhibits a reduction of 8.55% in peak overshoot when response is compared with Golob's [39] decomposed PID controller and a reduction of about 1.55% when compared to Golob's [39]Fuzzy PD+PI controller. The comparison clearly indicates that proposed controller shows a reduction in overshoot.

The results for proposed controller when compared to PID controller, FLC (non-optimized), indicate improvement in performance. The proposed controller also exhibits a reduction of about 92.96% in ISE as compared with PID and a reduction of about 84.53% as compared with FLC. The ITSE is reduced by 89.56% as compared with PID and 56.04% as compared with FLC. IAE shows a reduction of 88.31% as compared with PID and a reduction of 77.38% as compared with FLC. Similarly ITAE shows a reduction of 87.33% as compared with PID and reduction of about 70.38% as compared to FLC. The error indices indicate that proposed controller shows an overall improvement in set-point tracking when compared with PID or FLC.